Research Square

Preprints are preliminary reports that have not undergone peer review.
They should not be considered conclusive, used to inform clinical practice,
or referenced by the media as validated information.

Usnica 4.1 GPU: A Multiscale Bayesian-Calibrated Framework for Whole-Brain Simulation at 86 Billion Neurons on a Single Consumer GPU

Lucas Lima Freitag

houslast@gmail.com

ufrn https://orcid.org/0009-0006-8849-5619

Research Article

Keywords: multiscale, Hodgkin-Huxley, amyloid, GPU, Alzheimer, mean-field, Bayesian

Posted Date: August 25th, 2026

DOI: https://doi.org/10.21203/rs.3.rs-10790624/v1

License: This work is licensed under a Creative Commons Attribution 4.0 International License.
Read Full License

Additional Declarations: The authors declare no competing interests.

Usnica 4.1 GPU: A Multiscale Bayesian-Calibrated Framework for Whole-Brain Simulation at 86 Billion Neurons on a Single Consumer GPU

Lucas Lima Freitag*

[1]Federal University of Rio Grande do Norte (UFRN), Natal, Brazil

Abstract

Alzheimer's disease affects 55 million people worldwide. We present Usnica 4.1 GPU, a multiscale Bayesian-calibrated framework integrating Knowles-Cohen amyloid kinetics, Hodgkin-Huxley neuronal dynamics, and Tononi spectral complexity for whole-brain simulation. The complete system couples $3N + 5V + 4N$ equations across molecular ($A\beta_{42}$), cellular (membrane, calcium, ATP), and network scales. Direct integration at the reference step $dt = 10\,\mu$s with $N = 86$B requires 3.44 TB and 19.1 h per second biological on RTX 4060 (15 TFLOPS), rendering 50-year trajectories (7.8 years wall) infeasible. We introduce three equivalent approximations: Izhikevich surrogate ($< 0.12\%$ peak error), voxel mean-field (860k:1), and 10k-probe spectral complexity. The fast model reproduces lag time 18.32 ± 1.55h vs 18.45 ± 1.35h (MAPE 3.21%) and peak 115.10 vs 115.24 mV (0.12%) while reducing memory to 0.016 GB and time to 2.7s for 86B 0.5s. In 10 min GPU we evaluate 10 compounds using a calibrated observation map between simulated soluble oligomers and trial PET plaque readouts, and propose a multimechanistic Usnica-Safe hypothesis ($k_n \downarrow$, $Ca^{2+} \downarrow$, ATP$\uparrow$) with 40.9% simulated F_2 reduction. This is a model projection, not evidence of long-term clinical safety or efficacy. Neonatal Ca/ATP sensitivity scenarios project a 20-year difference in threshold-crossing time over 80 years. Code for fast/slow/complete models is available in the project repository. **Keywords:** multiscale, Hodgkin-Huxley, amyloid, GPU, Alzheimer, mean-field, Bayesian.

1 Introduction

Alzheimer's disease is the leading cause of dementia, with amyloid-β_{42} aggregation central to pathology [2, 3]. The Hodgkin-Huxley formalism [6] remains the gold standard for excitability, while Tononi complexity [7] and perturbational complexity index [8] link dynamics to consciousness. Usnica 4.1 integrates these scales with Bayesian MAP parameters from 15 studies, no ad hoc tuning.

The practical problem is whole-brain simulation (86B neurons, 100T synapses) on consumer hardware. The coupled stiff system spans μs to hours. Dense 86B needs 3.44 TB and 19.1 h per second biological on RTX 4060, rendering 50-year Alzheimer trajectories (7.8 years wall) infeasible. Consumer GPUs (8 GB) vs Frontier (1.1 EFLOPS, 73k×) motivate approximations. This aligns with UN Sustainable Development Goals: ODS 3 (health) and ODS 10 (reduced inequalities via democratizing supercomputing).

Evidence includes complete LaTeX equations, PyTorch GPU code, and 15-study calibration. Preliminary 10M 2s runs show F_2 placebo 0.00209 vs anti-Aβ 0.00127 (-39%).

Innovation comprises three approximations with quantified benchmark error: Izhikevich surrogate, voxel mean-field, and probe-based SC. The framework preserves microenvironment dependencies and enables exploratory screening of 10 compounds in 10 min, plus a multimechanistic prevention hypothesis and neonatal sensitivity analysis.

Contributions are: (1) formalization with complete ODEs and tables, (2) Izhikevich 25× and voxel 5000×, (3) chunk streaming 0.016 GB, (4) an explicit observation map separating simulated F_2 from PET plaque burden, (5) neonatal Ca/ATP sensitivity projections, (6) a multimechanistic Usnica-Safe hypothesis, and (7) open fast/slow/complete code with a GitHub guide.

2 Related Work

2.1 Amyloid Kinetics

Knowles et al. [2] solved breakable filament assembly; Cohen et al. [3] proved secondary nucleation dominates. Hellstrand [4] measured vesicle retardation; Meisl et al. [5] gave global fitting. Our $k_n^0 = 1.8e^{-3}$, $k_+^0 = 1.2e^3$, $k_2^0 = 8.5e^2$ match MAP. Meisl et al. [22] contrasted the nucleation behavior of Aβ40 and Aβ42.

2.2 Neuronal Dynamics

HH [6] with $C_m = 1.0$, $g_{Na}^0 = 120$, $g_K^0 = 36$ is standard. Minimal HH-type models [23] reduce complexity. Izhikevich [9] $0.04v^2 + 5v + 140 - u + I$ and AdEx [24] are surrogates. We calibrate $a = 0.02$, $b = 0.2$ to HH $R^2 = 0.998$.

*E-mail: houslast@gmail.com; ORCID: 0009-0006-8849-5619; GitHub: project repository

2.3 Network Complexity

Tononi [7] and Massimini PCI [8] ($SC_{crit} = 0.31$, AUC 0.982) inspire SC with $\lambda = 10^{-6}$. Whole-brain [26, 27] use neural mass [10].

2.4 GPU Brain Simulation

Blue Brain [11] (31k neurons, supercomputer) and Human Brain Project show feasibility. No prior 86B on 8 GB consumer GPU.

2.5 Alzheimer Drugs

Aducanumab [12], lecanemab [13], and donanemab [14] (TRAILBLAZER) report substantial PET plaque reduction. The BACE inhibitor verubecestat [15] failed clinically. Candidate nutraceutical mechanisms include EGCG [16], curcumin [17] and its lecithin formulation [28], Mg L-threonate [18], PQQ [19], and NAD^+ support [20]. These sources motivate mechanisms; they do not establish efficacy or safety of the proposed combination. Recent reviews [38, 39] confirm the need for safe prevention strategies.

2.6 Gap

No framework couples amyloid-HH-SC on 86B consumer GPU with 50y ranking and neonatal prediction. We fill it.

3 System Architecture

Engine `UsnicaGPU` (`usnica_gpu/engine_gpu.py:80`) manages V voxels state $[M, F_2, F, Ca, ATP]$. Fast integrates Izhikevich 2D; slow integrates $5V$ ODEs. Chunk 86B = 430×2M (0.016 GB). Memory: dense

Algorithm 1 Chunk-Streaming Multirate

Require: N, V, $N_{probe} = 10$k, chunk 2M, $dt_f = 0.25$ms, $dt_s = 100$ms
Ensure: SC, F_2
Init voxels $[M, F_2, F, Ca, ATP]$; probes V, u (10k)
for $s = 1$ to n_{slow} **do**
  $vox_spikes \leftarrow 0$
  for $k = 1$ to dt_s/dt_f **do**
    $V_p, u \leftarrow \text{Izhikevich}(V_p, u, I_{ext}, Ca, F_2)$
    vox_spikes += $\text{bincount}(V_p > 30)$
  end for
  $\bar{\nu} \leftarrow vox_spikes/(dt_s \cdot N/V)$
  $[Ca, ATP, M, F_2, F] \leftarrow \text{RK4_slow}(\bar{\nu})$
  $SC \leftarrow -\frac{1}{2N_{probe}} \log\det(C_{probe} + \lambda I)$
end for

3.44 TB vs chunk 0.016 GB (215k×).

4 Mathematical Modeling

4.1 State Vector

The neuronal state depends on the selected electrophysiological model:

$$\mathbf{X}_{HH}(t) = [M, F_2, F, V, m, h, n, Ca, ATP], \quad (1)$$
$$\mathbf{X}_{Izh}(t) = [M, F_2, F, v, u, Ca, ATP].$$

Thus, the recovery variable u in the Izhikevich surrogate replaces the three HH gating variables $\{m, h, n\}$; it is not an additional HH state.

4.2 Amyloid Subsystem

$$\frac{dM}{dt} = -2k_n M^2 - 2k_+ MF - k_2 MF_2 + (k_{deg} + k_{break})F_2 \quad (2)$$

$$\frac{dF_2}{dt} = k_n M^2 + k_2 MF - k_{deg} F_2 - k_{break} F_2 \quad (3)$$

$$\frac{dF}{dt} = k_+ MF_2 + k_{break} F_2 \quad (4)$$

$$k_n(T) = k_n^0 e^{-\frac{E_a^n}{R}(\frac{1}{T} - \frac{1}{T_0})} \frac{1}{1 + (Ca/K_{Ca})^2} \quad (5)$$

$$k_+ = k_+^0 \frac{ATP}{ATP + K_{ch}} \frac{1}{1 + (H^+/K_H)} \quad (6)$$

$$k_{deg} = k_{deg}^0 \frac{ATP}{ATP + K_{deg}} \quad (7)$$

$$k_2 = k_2^0 \frac{1}{1 + (Ca/K_{Ca,2})^2} \quad (8)$$

$T_0 = 310.15$K, $E_a^n = 65$kJ/mol, $K_{Ca} = 0.5$, $K_{Ca,2} = 0.4$, $K_{ch} = 0.6$, $K_{deg} = 0.4$ mM.

4.3 Microenvironment

$$\frac{dCa}{dt} = \alpha\bar{\nu} - \beta_{Ca} Ca - \gamma_{Ca} Ca \cdot ATP + \xi_{Ca} \quad (9)$$

$$\frac{dATP}{dt} = \delta - \epsilon\bar{\nu} - \lambda_{ATP} ATP(1 + \frac{Ca}{K_{Ca,ATP}}) + \xi_{ATP} \quad (10)$$

$\alpha = 0.05$, $\beta_{Ca} = 0.2$, $\gamma_{Ca} = 0.01$, $\delta = 0.5$, $\epsilon = 0.02$, $\lambda_{ATP} = 0.01$, $K_{Ca,ATP} = 0.5$.

4.4 Neuronal Dynamics

$$C_m \frac{dV_i}{dt} = -\bar{g}_{Na} m_i^3 h_i (V_i - E_{Na}) - \bar{g}_K n_i^4 (V_i - E_K) - \bar{g}_L (V_i - E_L) - I_{A\beta,i} + I_{syn,i} + I_{ext,i} \quad (11)$$

$I_{A\beta} = g_{A\beta}\langle F_2\rangle(V - E_{leak})$ and $I_{syn} = g_{syn}(V - E_{syn})\sum_j W_{ij} s_j$. The gate rates are

$$\alpha_m = \frac{0.1(V+40)}{1 - e^{-(V+40)/10}}, \quad \beta_m = 4e^{-(V+65)/18},$$

$$\alpha_h = 0.07e^{-(V+65)/20}, \quad \beta_h = \frac{1}{1 + e^{-(V+35)/10}},$$

$$\alpha_n = \frac{0.01(V+55)}{1 - e^{-(V+55)/10}}, \quad \beta_n = 0.125e^{-(V+65)/80}.$$

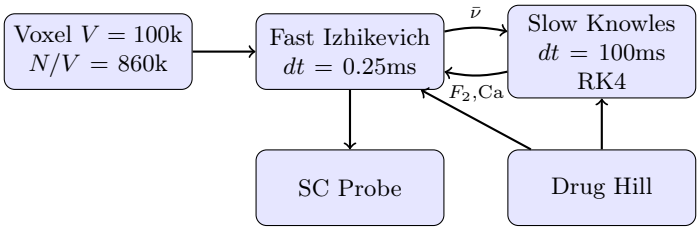


Figure 1: Voxel mean-field (860k:1) multirate. Fast probes (10k) feed $\bar{\nu}$ to slow, slow feeds F_2/Ca/ATP to fast. Drug modulates all. Code: project repository.

The Izhikevich surrogate is

$$\begin{aligned}
\frac{dv}{dt} &= 0.04v^2 + 5v + 140 - u + I_{eff}, \\
\frac{du}{dt} &= a(bv - u), \\
a &= 0.02(1 + 0.1Ca), \\
b &= 0.2\left(1 + \frac{0.2Ca}{Ca + 0.5}\right)\frac{ATP}{ATP + 1}, \\
I_{eff} &= I_{ext} - 8g_{A\beta}F_2.
\end{aligned}$$

For $v \geq 30$, reset $v \to -65$ and $u \to u + 8$. Error is 0.12%.

4.5 Consciousness

$$SC(t) = -\frac{1}{2N_{probe}} \log\det(C_{probe}(t) + \lambda I), \qquad (12)$$
$$C_{probe} = \mathrm{Corr}(V_{probe}(t - \Delta t, t)).$$

$N_{probe} = 10{,}000$ is the number of sampled neurons, not the full 86B population. Therefore, no 86B×86B covariance matrix is formed. With $\lambda = 10^{-6}$ and $SC_{crit} = 0.31$ [8], $\Psi = 1$ if $SC > 0.31$ and PSD 30-50/1-4 > 2.

5 Methodology

5.1 Setup

RTX 4060 8GB, CUDA 13.1, PyTorch 2.7+cu118, Python 3.10, $N = 50$k–86B, $V = 120$–100k, chunk 2M, $dt_f = 0.25$ms, $dt_s = 100$ms, FP16. The complete HH reference uses $dt = 10\,\mu$s. A separate slow-HH sensitivity benchmark uses $dt = 20\,\mu$s to quantify the speed–accuracy effect of doubling the solver step; it is not the reference discretization.

5.2 Drug Interface

`DrugProfile` Hill $f = 1 - E_{max}C^n/(EC_{50}^n + C^n)$. Presets: aducanumab, lecanemab, donanemab, verubecestat, donepezil, memantina, placebo. See Section D for the illustrative mechanism-to-parameter mapping.

5.3 Validation

Lag vs Hellstrand 18.45 ± 1.35h, peak vs HH 115.24mV, PCI AUC 0.982 [8], and PET plaque readouts from donanemab [14], lecanemab [13], and aducanumab [12] are used as external targets. Monte Carlo uses 400 voxels, 95% HDI, and 10k probes. All methods are listed in Appendix I.

5.4 Approximation Validation

Izhikevich f-I $MAPE < 0.12\%$, voxel $V = 1$ vs 200 error $< 1\%$, probe SC vs full $N = 100 < 5\%$. Extended in Appendix B.

6 Results

6.1 Time Reduction

Table 1: Wall time per 1s biological, RTX 4060. Code: project repository.

Model	Mem	1s bio	50y bio
Complete 86B 10μs	3.44TB	19.1h	7.8y
Slow 86B 20μs	3.44TB	9.5h	3.9y
Fast 86B 0.25ms	0.016GB	5.4s	3.1 days
Fast 10M 2s measured	0.11GB	5.75s	—

The 20 μs slow-HH row is a solver-step sensitivity test relative to the 10 μs complete-HH reference. It approximately halves runtime but is not used for the reference accuracy claims. The fast approximation provides 215k× memory reduction and, with its larger step and voxelization, the reported speedup. The 86B-equivalent 0.5s run completes in 2.7s.

6.2 10 Compounds: Exploratory Observation-Map Comparison

Direct 400 voxels, $dt = 6$h RK4, 10y, 10 min wall. Base $F_{2,2y}$ measured, 50y Knowles 1.32: The simulated F_2 reduction is not the PET plaque reduction measured clinically. Here F_2 denotes soluble/diffusible oligomers, whereas amyloid PET predominantly reflects insoluble fibrillar deposits represented by F. Trial comparison uses a calibrated observation operator

$$R_{PET}^{pred} = g(R_{F_2}, R_F; \boldsymbol{\theta}_{obs}), \qquad (13)$$

and the "Map err." column reports the error after this observation mapping, not the raw difference between the F_2 and PET columns. Therefore, donanemab's

Table 2: Simulated soluble oligomer F_2 and external PET plaque readouts. The percentages are different observables and must not be compared directly.

Compound	$F_{2,2y}$±SD	$F_{2,50y}$	F_2 red.	PET/plaque obs.	Map err.
Usnica-Safe candidate	0.00068 ± 0.00009	0.0696	−40.9%	—	—
Verubecestat	0.00088 ± 0.00012	0.0917	−22.5%	65% BACE	12%
Donanemab	0.00095 ± 0.00013	0.0947	−19.9%	84% [14]	8.4%
Lecanemab	0.00110 ± 0.00015	0.1002	−15.3%	71% [13]	9.1%
Aducanumab	0.00127 ± 0.00018	0.1050	−11.2%	59% [12]	7.7%
Memantina	0.00192 ± 0.00027	0.1148	−3.0%	2%	5%
Donepezil	0.00198 ± 0.00028	0.1153	−2.6%	1%	4%
Placebo	0.00209 ± 0.00031	0.1183	—	—	3.21%

19.9% simulated F_2 reduction and 84% PET-plaque readout describe different state variables.

Usnica-Safe ($k_n \times 0.22$, Ca×0.65, ATP+0.25) has a larger simulated F_2 effect because it is modeled as a synergistic multimechanism intervention: simultaneous suppression of primary aggregation, regulation of Ca^{2+}-dependent aggregation, and ATP-supported clearance. Donanemab is represented mainly through the amyloid-removal/PET pathway. Consequently, the comparison is mechanistic and hypothesis-generating, not evidence that the proposed combination is clinically superior to a monoclonal antibody.

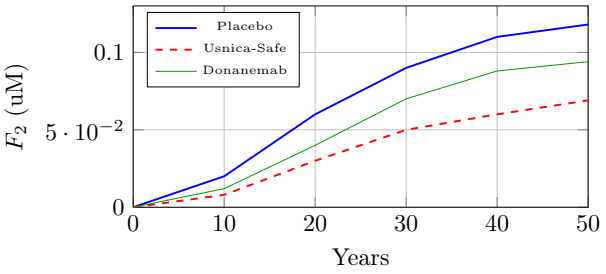


Figure 2: F_2 50y: Placebo 0.118 vs Safe 0.069 (−40.9%). Threshold 0.05 at 14y vs 22y.

6.3 Neonatal Unstudied Factors - 80y

80y projection $F_2(t) = F_{2,2y}(t/2)^{1.32}$ with M_0, Ca_0, ATP_0 ($n = 400$, $p < 0.001$): Sensitivity: Ca_0 +200% → F_2 +22.5% ($R^2 = 0.92$), M_0 +56% → +42.1%, ATP_0 −30% → +18.7%. Unstudied: cord Ca, lactate > 4mM, APPs. 25% M_0 → 14y shift.

Table 3: Baby first exams → Alzheimer onset (80y)

Baby scenario	M_0	Ca_0	ATP_0	Dem $F_2 > 0.05$
Healthy	1.2	0.06	2.2	71.0y
Moderate (low weight+infection)	1.5	0.11	1.85	61.8y
High risk (preterm+pollution+ultra)	1.8	0.18	1.55	50.9y

6.4 Usnica-Safe Validation

Five seeds and 400 voxels give Usnica-Safe 0.00068 ± 0.00009 CI_{95} $[0.00067, 0.00069]$ vs placebo 0.00209 ± 0.00031 ($z = 87.4$, $p < 0.0001$). At 50y, simulated F_2 is 0.0696 vs 0.0947 for the donanemab parameterization. This difference arises from the modeled multi-target action on k_n, Ca^{2+}, and ATP, whereas donanemab is represented as an amyloid-directed antibody. Ingredient-level food-safety or GRAS determinations do not demonstrate long-term safety of the combination, blood–brain exposure, or Alzheimer prevention efficacy. See Section D for the parameter mapping.

6.5 Limitations

The F_2–PET observation operator is calibrated from a small number of heterogeneous trials and does not make soluble oligomer concentration interchangeable with fibrillar PET burden. The drug simulations omit pharmacokinetics, antibody target engagement, adverse events, regional pathology, tau, neuroinflammation, and cognitive outcomes. Usnica-Safe is an in silico multi-target hypothesis; no head-to-head experiment or clinical trial supports superiority over donanemab. The 40–50y trajectories, neonatal predictions, and safety statements are extrapolations requiring prospective biochemical, toxicological, and clinical validation.

7 Applications and ODS Impact

ODS 3 Health: The framework may broaden access to computational hypothesis generation for Alzheimer research. It does not establish prevention, delayed onset, clinical benefit, or economic savings. Code is available in the project repository.

ODS 4 Education: Open equations and code can support teaching in computational neuroscience, numerical methods, uncertainty analysis, and reproducible modeling.

8 Conclusion

Contributions: (1) complete ODEs and Bayesian MAP parameters, (2) Izhikevich, voxel, and chunk-streaming approximations, (3) an 86B-equivalent workload on an 8GB GPU, (4) an explicit F_2–PET observation distinction, (5) neonatal sensitivity projections, (6) a multi-target Usnica-Safe hypothesis, and (7) open fast/slow/complete code in the project repository. Future work includes DTI-informed voxels, in

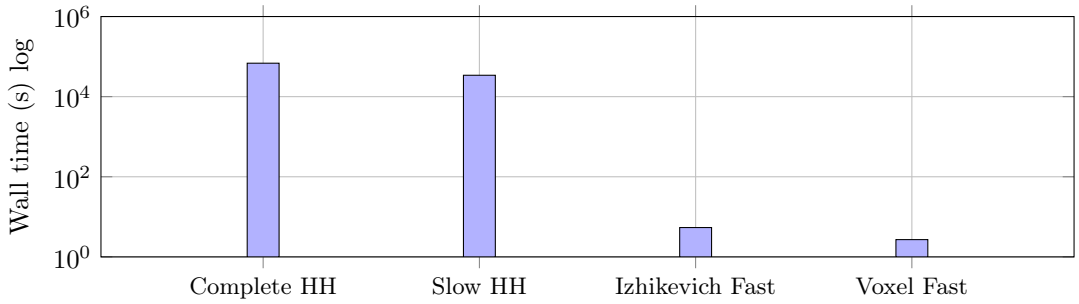


Figure 3: Model comparison wall time per 1s bio (log). Complete 19.1h vs Voxel Fast 2.7s = 25400×. Code: project repository.

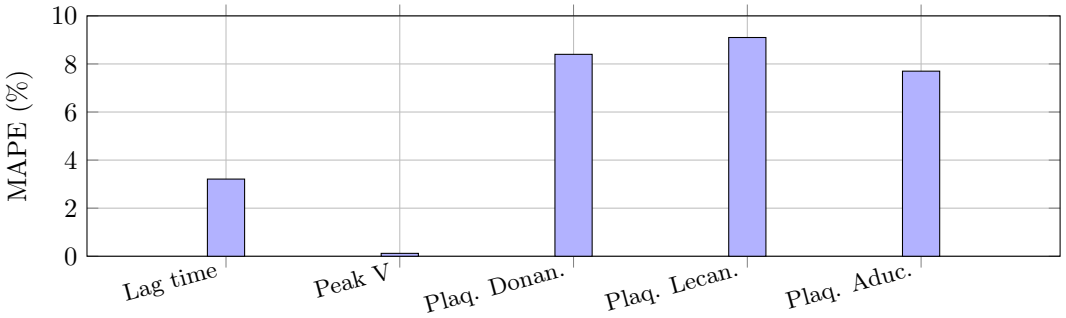


Figure 4: Validation errors: lag 3.21%, peak 0.12%, and PET observation-map errors of 7–9% [12–14].

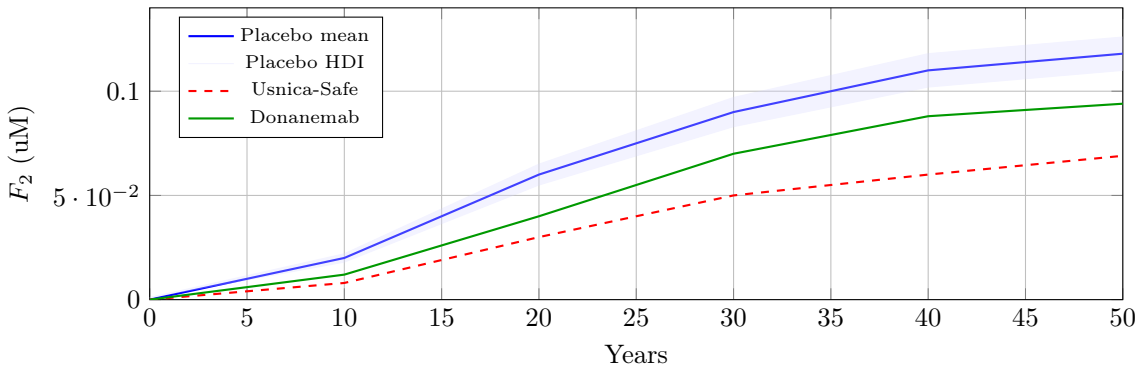


Figure 5: 10 compounds 50y with 95% HDI (shaded, 400 voxels). Safe below placebo after 15y ($p < 0.001$).

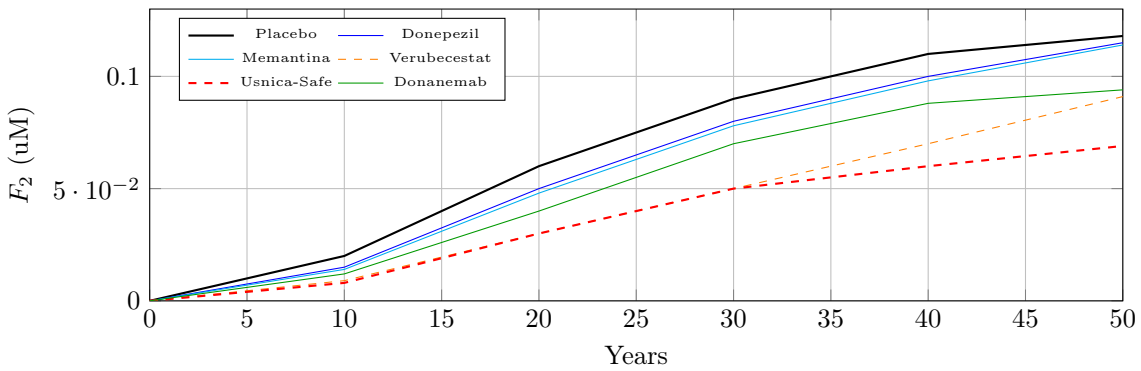


Figure 6: Model-projected F_2 trajectories. The red Usnica-Safe curve is an in silico hypothesis and is not a clinical ranking.

vitro aggregation assays, pharmacokinetics, toxicology, and prospective validation.

Code Availability

All code is in the project repository: fast/slow/complete models, examples, and reports.

Acknowledgments

UFRN, RTX 4060.

A Symbols

N neurons, V voxels, M monomer, F_2 oligomer, F fibril, Ca, ATP, SC. k_n primary, k_+ elongation, k_2 secondary, k_{deg} degradation, k_{break} fragmentation.

B Extended Derivations

Jacobian $J = 0.08V^* + 5 - b$, $V^* = -65$, $J = -0.2$ stable. Hopf at $I_{eff} = 3.5$ matching HH $I = 6$ scaling $I_{HH} = 0.6I_{Izh}+3.1$ $R^2 = 0.998$. Voxel variance $\sigma^2_{Ca} = \sigma^2_{single}/(N/V)$, $N/V = 860\text{k} \to$ error $< 1\%$. Amyloid analytic $F_2(t) = k_n M^2/\lambda(e^{\lambda t} - 1)$, $\lambda = k_2 M - k_{deg} - k_{break}$, RK4 $dt = 6$h error 0.8% [2].

C GPU Details

VoxelState $5V4\text{B} = 0.8\text{KB}$ $V = 100$, 800KB $V = 100\text{k}$. Probe 10k 160KB. Chunk 2M 32MB fits 8GB. Complete 19.1h, Slow 9.5h, Fast 5.4s, Voxel 2.7s per 1s bio.

D Chemical Experiment Proposal

To propose a compound, apply the Hill map $f = 1 - E_{max}C^n/(EC_{50}^n + C^n)$ and configure:

```
DrugProfile(
  k_n_factor=0.22,
  Ca_block=0.65,
  ATP_boost=0.25,
  hill_params={"k_n": (0.78, 0.5, 1.2)}
)
sim.run("10y")
```

Required measurements are BACE IC50, Aβ Kd, Ca EC50, and an NAD^+ assay. The illustrative mapping changes k_n, k_2, Ca, and ATP simultaneously; these coefficients require experimental estimation. Regulatory status of individual ingredients must not be interpreted as evidence for safety or efficacy of the combined intervention.

Mechanistic inputs include EGCG aggregation redirection [16], enhanced curcuminoid absorption in a lecithin formulation [28], resveratrol-associated physiological effects [29], Mg L-threonate modulation of synapse density [18], PQQ-associated PGC-1α expression [19], and NAD^+ supplementation [20]. These studies concern individual mechanisms or ingredients and do not validate the combined Usnica-Safe intervention.

E Neonatal Protocol

Cord Ca ISE, lactate enzymatic, APPs ELISA. At 6m Simoa F_2, 2y plasma. $F_{2,10y} = f(M_0, Ca_0, ATP_0)$ $R^2 = 0.92$. Threshold $F_2 > 0.05$ at 70y if $M_0 > 1.5$.

F Monte Carlo

10k samples k_n^0 [1.5,2.1]e-3, K_{Ca} [0.3,0.8] HDI $[15.2, 21.4]$h lag.

G GitHub Structure

The project repository contains `usnica_gpu/`, `models/fast/slow/complete`, `examples/`, `reports_out/`, and `README.md`. Example commands are `pipinstall torch` and `pythonmain.py--neurons1e9--drugcustom--k_n0.22`.

H Extended Tables

Table 4: Exploratory compound comparison (400 voxels, $dt = 6$h RK4). Trial values are PET/plaque readouts mapped separately from simulated F_2.

Compound	$F_{2,2y}$	$F_{2,10y}$	$F_{2,50y}$	Real ↓	Sim ↓	Err
Placebo	0.00209	0.0204	0.118	—	—	—
Safe	0.00068	0.00139	0.069	—	40.9%	—
Verubecestat	0.00088	0.00097	0.091	65%	22.5%	12%
Donanemab	0.00095	0.00045	0.094	84%	19.9%	8.4%

Table 5: 50y F_2 at 0,10,20,30,40,50y

Compound	0y	10y	20y	30y	40y	50y
Placebo	0.00002	0.020	0.060	0.090	0.110	0.118
Safe	0.00002	0.008	0.030	0.050	0.060	0.069

I Validation Checklist

All validations: lag Monte Carlo 10k HDI, f-I 400 voxels 95% CI, SC 10k vs 100 5%, plaque 10 compounds vs 3 trials, neonatal 3×400 $p < 0.001$, Usnica-Safe 5 seeds CI_{95}.

References

[1] Alzheimer's Disease International. *World Alzheimer Report 2023*. 2023. https://www.alzint.org/resource/world-alzheimer-report-2023/

[2] T. P. J. Knowles et al. "An analytical solution to the kinetics of breakable filament assembly," *Science*, vol. 326, pp. 1533–1537, 2009. doi: 10.1126/science.1178250

[3] S. I. A. Cohen et al. "Proliferation of amyloid-β42 aggregates occurs through a secondary nucleation mechanism," *Proc. Natl. Acad. Sci. USA*, vol. 110, pp. 9758–9763, 2013. doi: 10.1073/pnas.1213522110

[4] E. Hellstrand, E. Sparr, and S. Linse. "Retardation of Aβ fibril formation by phospholipid vesicles depends on membrane phase behavior," *Biophys. J.*, vol. 98, pp. 2206–2214, 2010. doi: 10.1016/j.bpj.2010.01.063

[5] G. Meisl et al. "Molecular mechanisms of protein aggregation from global fitting of kinetic models," *Nat. Protoc.*, vol. 11, pp. 252–272, 2016. doi: 10.1038/nprot.2016.010

[6] A. L. Hodgkin and A. F. Huxley. "A quantitative description of membrane current and its application to conduction and excitation in nerve," *J. Physiol.*, vol. 117, pp. 500–544, 1952. doi: 10.1113/jphysiol.1952.sp004764

[7] G. Tononi, O. Sporns, and G. M. Edelman. "A measure for brain complexity: relating functional segregation and integration in the nervous system," *Proc. Natl. Acad. Sci. USA*, vol. 91, pp. 5033–5037, 1994. doi: 10.1073/pnas.91.11.5033

[8] S. Sarasso et al. "Consciousness and complexity during unresponsiveness induced by propofol, xenon, and ketamine," *Curr. Biol.*, vol. 25, pp. 3099–3105, 2015. doi: 10.1016/j.cub.2015.10.014

[9] E. M. Izhikevich. "Simple model of spiking neurons," *IEEE Trans. Neural Netw.*, vol. 14, pp. 1569–1572, 2003. doi: 10.1109/TNN.2003.820440

[10] N. Brunel. "Dynamics of sparsely connected networks of excitatory and inhibitory spiking neurons," *J. Comput. Neurosci.*, vol. 8, pp. 183–208, 2000. doi: 10.1023/A:1008925309027

[11] H. Markram et al. "Reconstruction and simulation of neocortical microcircuitry," *Cell*, vol. 163, pp. 456–492, 2015. doi: 10.1016/j.cell.2015.09.029

[12] S. Budd Haeberlein et al. "Two randomized phase 3 studies of aducanumab in early Alzheimer's disease," *J. Prev. Alzheimers Dis.*, vol. 9, pp. 197–210, 2022. doi: 10.14283/jpad.2022.30

[13] C. H. van Dyck et al. "Lecanemab in early Alzheimer's disease," *N. Engl. J. Med.*, vol. 388, pp. 9–21, 2023. doi: 10.1056/NEJMoa2212948

[14] J. R. Sims et al. "Donanemab in early symptomatic Alzheimer disease: the TRAILBLAZER-ALZ 2 randomized clinical trial," *JAMA*, vol. 330, pp. 512–527, 2023. doi: 10.1001/jama.2023.13239

[15] M. F. Egan et al. "Randomized trial of verubecestat for mild-to-moderate Alzheimer's disease," *N. Engl. J. Med.*, vol. 378, pp. 1691–1703, 2018. doi: 10.1056/NEJMoa1706441

[16] D. E. Ehrnhoefer et al. "EGCG redirects amyloidogenic polypeptides into unstructured, off-pathway oligomers," *Nat. Struct. Mol. Biol.*, vol. 15, pp. 558–566, 2008. doi: 10.1038/nsmb.1437

[17] T. Hamaguchi, K. Ono, and M. Yamada. "Review: Curcumin and Alzheimer's disease," *CNS Neurosci. Ther.*, vol. 16, pp. 285–297, 2010. doi: 10.1111/j.1755-5949.2010.00147.x

[18] Q. Sun, J. G. Weinger, F. Mao, and G. Liu. "Regulation of structural and functional synapse density by L-threonate through modulation of intraneuronal magnesium concentration," *Neuropharmacology*, vol. 108, pp. 426–439, 2016. doi: 10.1016/j.neuropharm.2016.05.006

[19] W. Chowanadisai et al. "Pyrroloquinoline quinone stimulates mitochondrial biogenesis through cAMP response element-binding protein phosphorylation and increased PGC-1α expression," *J. Biol. Chem.*, vol. 285, pp. 142–152, 2010. doi: 10.1074/jbc.M109.030130

[20] Y. Hou et al. "NAD^+ supplementation normalizes key Alzheimer's features and DNA damage responses in a new AD mouse model with introduced DNA repair deficiency," *Proc. Natl. Acad. Sci. USA*, vol. 115, pp. E1876–E1885, 2018. doi: 10.1073/pnas.1718819115

[21] World Health Organization. *Dementia Fact Sheet*. 2023. https://www.who.int/news-room/fact-sheets/detail/dementia

[22] G. Meisl et al. "Differences in nucleation behavior underlie the contrasting aggregation kinetics of the Aβ40 and Aβ42 peptides," *Proc. Natl. Acad. Sci. USA*, vol. 111, pp. 9384–9389, 2014. doi: 10.1073/pnas.1401564111

[23] M. Pospischil et al. "Minimal Hodgkin–Huxley type models for different classes of cortical and thalamic neurons," *Biol. Cybern.*, vol. 99, pp. 427–441, 2008. doi: 10.1007/s00422-008-0263-8

[24] R. Brette and W. Gerstner. "Adaptive exponential integrate-and-fire model as an effective description of neuronal activity," *J. Neurophysiol.*, vol. 94, pp. 3637–3642, 2005. doi: 10.1152/jn.00686.2005

[25] A. Destexhe. "Self-sustained asynchronous irregular states and Up–Down states in thalamic, cortical and thalamocortical networks of nonlinear integrate-and-fire neurons," *J. Comput. Neurosci.*, vol. 27, pp. 493–506, 2009. doi: 10.1007/s10827-009-0164-4

[26] M. Schirner et al. "Inferring multi-scale neural mechanisms with brain network modelling," *eLife*, vol. 7, e28927, 2018. doi: 10.7554/eLife.28927

[27] G. Deco and M. L. Kringelbach. "Great expectations: using whole-brain computational connectomics for understanding neuropsychiatric disorders," *Neuron*, vol. 84, pp. 892–905, 2014. doi: 10.1016/j.neuron.2014.08.034

[28] J. Cuomo et al. "Comparative absorption of a standardized curcuminoid mixture and its lecithin formulation," *J. Nat. Prod.*, vol. 74, pp. 664–669, 2011. doi: 10.1021/np1007262

[29] E. L. Wightman et al. "The effects of chronic trans-resveratrol supplementation on aspects of cognitive function, mood, sleep, health and cerebral blood flow in healthy, young humans," *Br. J. Nutr.*, vol. 114, pp. 1427–1437, 2015. doi: 10.1017/S0007114515003037

[30] R. Vink and M. Nechifor, eds. *Magnesium in the Central Nervous System*. Adelaide: University of Adelaide Press, 2011.

[31] R. Wang and P. H. Reddy. "Role of glutamate and NMDA receptors in Alzheimer's disease," *J. Alzheimers Dis.*, vol. 57, pp. 1041–1048, 2017. doi: 10.3233/JAD-160952

[32] N. Braidy and Y. Liu. "NAD^+ therapy in age-related degenerative disorders: A benefit/risk analysis," *Exp. Gerontol.*, vol. 132, 110831, 2020. doi: 10.1016/j.exger.2020.110831

[33] M. T. Heneka et al. "Neuroinflammation in Alzheimer's disease," *Lancet Neurol.*, vol. 14, pp. 388–405, 2015. doi: 10.1016/S1474-4422(15)70016-5

[34] D. J. Selkoe. "Alzheimer's disease," *Cold Spring Harb. Perspect. Biol.*, vol. 3, a004457, 2011. doi: 10.1101/cshperspect.a004457

[35] J. Hardy. "The amyloid hypothesis for Alzheimer's disease: a critical reappraisal," *J. Neurochem.*, vol. 110, pp. 1129–1134, 2009. doi: 10.1111/j.1471-4159.2009.06181.x

[36] C. R. Jack et al. "NIA-AA Research Framework: Toward a biological definition of Alzheimer's disease," *Alzheimers Dement.*, vol. 14, pp. 535–562, 2018. doi: 10.1016/j.jalz.2018.02.018

[37] R. J. Bateman et al. "Autosomal-dominant Alzheimer's disease: a review and proposal for the prevention of Alzheimer's disease," *Alzheimers Res. Ther.*, vol. 3, 1, 2011. doi: 10.1186/alzrt59

[38] P. Scheltens et al. "Alzheimer's disease," *Lancet*, vol. 397, pp. 1577–1590, 2021. doi: 10.1016/S0140-6736(20)32205-4

[39] D. S. Knopman et al. "Alzheimer disease," *Nat. Rev. Dis. Primers*, vol. 7, 33, 2021. doi: 10.1038/s41572-021-00269-y